

# Parameter calibration of a modified hyperbolic model for sands using pressuremeter test data

Oztoprak, Sadik

*Department of Civil Engineering, Istanbul University, 34320 Istanbul, Turkey, oztoprak@istanbul.edu.tr*

Bolton, Malcolm. D.

*Schofield Centre, Department of Engineering, University of Cambridge, Cambridge CB3 0EL, UK, mdb@eng.cam.ac.uk*

**Keywords:** Sand, stiffness, shear modulus degradation, hyperbolic model, pressuremeter test

**ABSTRACT:** The degradation of shear modulus causes non-linearity before plastic yielding, and this needs to be taken into account in deformation analyses for the performance-based design of geotechnical structures. In this respect, this paper demonstrates the simulations of pressuremeter tests via a non-linear elastic perfectly plastic soil model. A modified hyperbolic model was adopted for the pre-failure part of the stress-strain behaviour, and the Mohr Coulomb soil model was implemented for modelling the post-failure behaviour in FLAC3D. Computed pressure-displacement curves at the cavity wall matched very well with the curves of self boring pressuremeter tests carried out in Thanet sand. A new pressuremeter disturbance correction is used successfully as a means of adjusting and updating the shear modulus. The analysis reveals that this approach is essential for estimating the initial lateral earth pressure coefficient, and is capable of refining the selection of new degradation parameters in the modified hyperbolic model using pressuremeter rebound loops, and of refining values of friction and dilation angles from initial expansion and final contraction curves. Using the modified hyperbolic model in conjunction with pressuremeter test data enables not only calibration, but also optimization of parameters. The simulation of a pressuremeter test enables the engineer to obtain an appropriate combination of soil parameters which can later be utilized to analyze geotechnical structures through the same calibrated model.

## 1. INTRODUCTION

Deformations of sandy soils around typical geotechnical structures display small to medium strain magnitudes under static loading. In this strain range the soil exhibits non-linear stress-strain behaviour which should be incorporated in any deformation analysis. However, there are some limitations on the incorporation of non-linear elasticity into numerical models because of their complexity and the requirement for special testing procedures. Engineers in practice generally analyse with sands prior to failure using a linear elastic soil model, with a shear modulus that is assumed to be constant. Furthermore, due to the great difficulty of recovering undisturbed samples of sands, and the sophisticated nature of the required tests, very few practising engineers undertake the laboratory testing necessary to validate the selection of any such constant stiffness modulus. They often estimate the shear modulus from SPT or CPT data, using weak empirical correlations. Pressuremeter tests can offer much better reliability, but it has not previously been easy to extract meaningful soil parameters from the data. This paper aims to show a practical methodology for doing so.

The degradation of shear modulus with strain has been observed in soil dynamics since the 1970s and a great deal of stiffness data for sands has been published for the purpose of judging amplification factors and liquefaction risk. The dependence of secant shear modulus  $G$  on strain amplitude was illustrated for dynamic loading by a number of researchers using the resonant column test or improved triaxial tests (Seed and Idriss, 1970; Hardin and Drnevich, 1972; Iwasaki et al., 1978; Kokusho, 1980; Tatsuoka and Shibuya, 1991; Yamashita and Suzuki, 1994). The same concept has been applied to static behaviour from the mid 1980s (Jardine et al., 1986, Atkinson and Salfors, 1991; Simpson, 1992). The original relation for maximum shear modulus  $G_o$  proposed by Hardin and Richart (1963) was modified for strain dependence in Eq. 1 which was formulated to be dimensionless:

$$G = A(\gamma) \cdot F(e) \cdot p_a \cdot (p' / p_a)^{m(\gamma)} \quad (1)$$

where  $A(\gamma)$  and  $m(\gamma)$  are strain dependent parameters,  $p_a$  is the atmospheric pressure,  $p'$  is mean effective stress, and  $F(e)$  is a void ratio function which for round sands

was defined as  $(2.17 \cdot e)^2 / (1 + e)$ . Generally,  $m(\gamma)$  is taken 0.5 for the  $G_o$  calculation. On the other hand, to model shear modulus reduction, most researchers suggested different versions of hyperbolae, such as Ramberg and Osgood (1943), Hardin and Drnevich (1972), Ishibashi, and Zhang (1993), Fahey and Carter (1993), Darendeli, (2001) and Yi (2010). Jardine et al (1986), however, proposed a polynomial to fit their data.

Oztoprak and Bolton (2011) recently constructed a database of shear modulus degradation curves from 454 tests in order to produce best-fit functional relationships for shear stiffness of sandy soils. Obtaining a unique S-shaped curve of shear modulus degradation, a modified hyperbolic relationship was fitted to the data. The new curve fitting parameters, elastic threshold strain ( $\gamma_e$ ) and characteristic reference strain ( $\gamma_r$ ), were defined as functions of soil type and stress level, promising a practical way of incorporation into numerical methods.

This paper demonstrates the implementation of this newly modified hyperbolic model for modelling pressuremeter tests using FLAC3D finite difference software. Its performance was tested on three self boring pressuremeter tests in Thanet sand. The influence of soil parameters, singly and in combination, is discussed.

## 2. STIFFNESS BASED SOIL MODELING

### 2.1 Modified hyperbolic model

A large amount of laboratory stiffness data for sandy soils has been published since the 1970s to identify the maximum shear modulus and the rate of shear modulus reduction with shear strain in particular soils. With the available stiffness data, Oztoprak and Bolton (2011) refined the modified hyperbolic relationship of Darendeli (2001) to create a unique S-shaped curve of shear modulus degradation  $G/G_o$  given in eq. (2):

$$\left( \frac{G}{G_o} \right) = \frac{1}{1 + \left( \frac{\gamma - \gamma_e}{\gamma_r} \right)^a} \quad (2)$$

where  $\gamma_e$ ,  $\gamma_r$  and  $a$  are as defined in eqs. (3) to (5):

$$\gamma_r (\%) = 0.01 \cdot U_c^{-0.3} \cdot \left( \frac{p'}{p_a} \right) + 0.08 \cdot e \cdot I_D \quad (3)$$

$$\gamma_e (\%) = 0.0002 + 0.012 \cdot \gamma_r (\%) \quad (4)$$

$$a = U_c^{-0.075} \quad (5)$$

Three curve-fitting parameters were used: elastic threshold strain ( $\gamma_e$ ), reference strain ( $\gamma_r$ ) and curvature parameter ( $a$ ). Reference strain is the post-elastic shear strain required to reduce  $G/G_o$  to 0.5 and this was found to depend on soil type (uniformity coefficient  $U_c$ ), soil state (voids ratio  $e$  and relative density  $I_D$ ) and on the mean effective stress ( $p'$ ). The elastic threshold strain was found to be linked to the reference strain, and the curvature parameter was found to be a function of the uniformity coefficient. Before Oztoprak and Bolton (2011), only Menq (2003) had made an attempt to include  $U_c$  into the formulation of  $G$  degradation.

With the elastic stiffness data, Oztoprak and Bolton (2011) proposed a version of empirical relation for the initial shear modulus,  $G_o$ :

$$G_o = \frac{5760 \cdot p_a}{(1 + e)^3} \cdot \left( \frac{p'}{p_a} \right)^{0.5} \quad (6)$$

Here, the simpler voids ratio function  $1/(1+e)^3$  was preferred to that of Hardin and Richart (1963) since

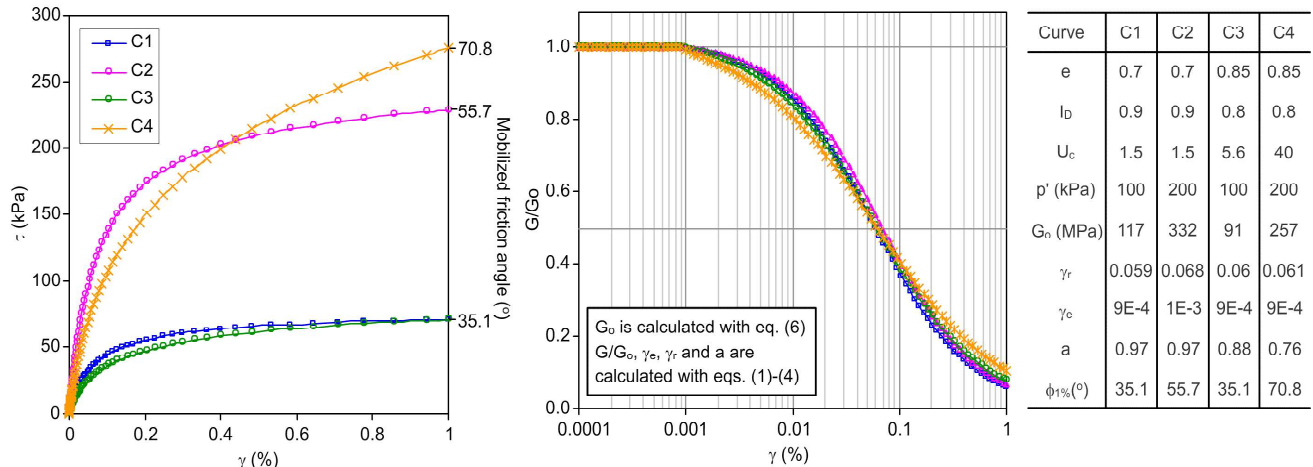


Figure 1. Evolution of shear stress-shear strain and normalized shear modulus-shear strain curves by using the modified hyperbolic model for different soils and stresses

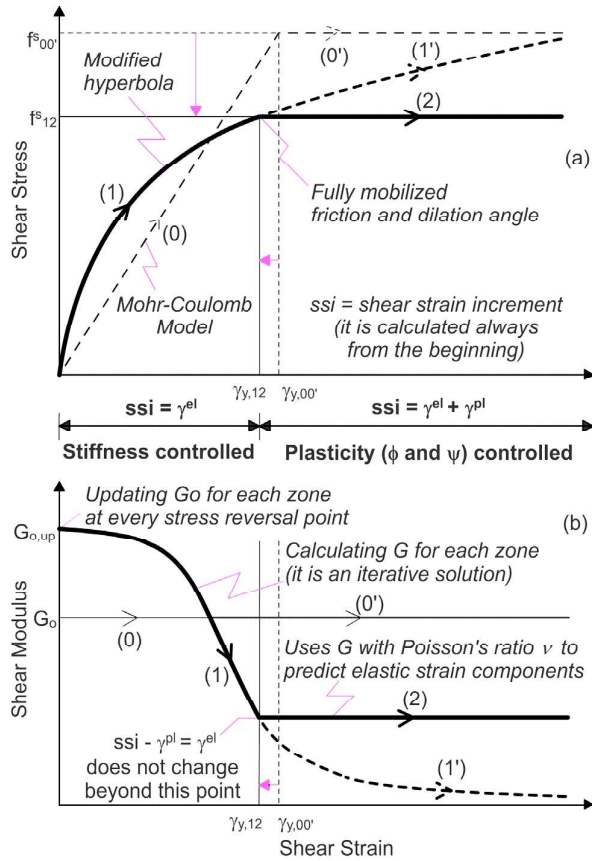


Figure 2. Schematic representation of shear stress-shear strain response of non-linear elastic perfectly plastic model used for any element and mid-expansion phase in FLAC3D

it also reduced scatter. According to Oztoprak and Bolton (2011),  $G_o$  can be estimated within a factor of 1.6 for one standard deviation. Additionally, the new empirical expression for shear modulus reduction  $G/G_o$  is shown to make predictions that are accurate within a factor of 1.13 for one standard deviation of random error.

Fig. 1 demonstrates the performance of the modified hyperbolic model. As noticed, the model has the capability to evolve the normalized shear modulus curves responsively when the soil type and stress change. Note that a limiting  $\phi$  value is separately invoked to exclude unrealistically high large-strain values predicted by (2), as with curve C4 beyond  $\gamma \approx 0.4\%$  in Fig. 1.

## 2.2 Incorporating the new model in FLAC3D

FLAC3D is based on a continuum finite difference discretization using a Lagrangian approach. It offers a wide range of capabilities (e.g. large strains, anisotropy) to solve complex problems in geomechanics. The program offers a number of constitutive models for geomaterials. These can be modified by the user through a macro programming language (FISH) which is embedded within FLAC3D. New constitutive models can also be incorporated.

In this paper, it was preferred to modify the strain-hardening/softening (SH) model to improve its performance in the small strain range. The SH model allows representation of nonlinear material softening and hardening behaviour based on prescribed variations of the Mohr-Coulomb (MC) model properties (cohesion, friction, dilation, tensile strength) as functions of the plastic shear strain which are not an output in the MC model. To incorporate the modified hyperbolic model in FLAC3D, a FISH function was written to represent the reduction of shear modulus during straining up to failure. Fig. 2a shows the stress-strain curve obtained by using the modified hyperbolic model for the pre-failure part and the perfectly plastic yield limit for the post-failure part of the stress-strain behaviour in FLAC3D. Fig. 2b exhibits the corresponding shear modulus-shear strain relation of the model. The original shear stress-strain and shear modulus-strain curves (curve '0') of the MC model can also be followed in Fig. 2.

The MC (also the SH) model is used for materials that yield when subjected to shear loading; a shear yield function and a non-associated shear flow rule are used. In addition, the failure envelope for the model is characterized by a tensile yield function with associated flow rule. The yield stress ( $f_s$ ) depends on the major and minor principal stresses ( $\sigma_1$  and  $\sigma_3$  respectively) only; the intermediate principal stress ( $\sigma_2$ ) has no effect on yield. In the original MC model (also the SH model), the stress-strain curve is linear to the point of yield (curve '0' in Fig.2); in that range, the strain is elastic only:  $\gamma = \gamma^p$ . After yield, the total strain is composed of elastic and plastic parts:  $\gamma = \gamma^e + \gamma^p$ . The stress to cause shear failure in the FLAC3D MC model is defined as

$$f^S = \sigma_1 - \sigma_3 N_\phi + 2c\sqrt{N_\phi} \quad (7)$$

where

$$N_\phi = (1 - \sin \phi) / (1 + \sin \phi) \quad (8)$$

Here;  $c$  is cohesion, and  $\phi$  is friction angle. Beyond peak strength, soil plasticity was invoked, using Rowe's stress-dilatancy with constant friction angle ( $\phi$ ) and dilation angle ( $\psi$ ). The plastic potential is given by

$$g^S = \sigma_1 - \sigma_3 N_\psi \quad (9)$$

where

$$N_\psi = (1 - \sin \psi) / (1 + \sin \psi) \quad (10)$$

The developed model can be defined as a modified hyperbolic model using MC yield surface. The procedure of the adopted model is given below:

- i. A calculation step starts with a given  $G_o$  as updated by eq. (6); calculated incremental shear strain ( $ssi$ ) values are stored after the calculation for each zone.
- ii. Corresponding shear modulus values are obtained from the calculated modulus reduction curve through a FISH function using the stored  $ssi$  values. The function always uses the elastic part ( $\gamma_e$ ) of the  $ssi$  as the value of  $\gamma$  to be used in eq. (2). It means that  $ssi = \gamma_e$  before yielding and  $ssi = \gamma_e + \gamma_p$  afterwards.
- iii. Gridpoint displacements are updated with the new incremental strains. The program proceeds to the next loading stage.

### 3. PRESSUREMETER MODELING

#### 3.1 Introduction

The pressuremeter has been widely used to measure soil properties, especially stiffness and strength. Since the 1970's, both numerical and analytical solutions based on different soil models have been proposed to get shear strength and stress-strain characteristics from pressuremeter tests. These solutions generally assume conditions of radial symmetry and invoke the expansion and contraction of a cylindrical cavity.

Hughes et al. (1977) and Manassero (1989) proposed similar methods of determining the angle of effective internal friction  $\phi$  and the angle of dilatation  $\psi$  from pressuremeter test data in sand. In adopting a more rigorous approach, the authors assumed that sand behaves as a dilatant elastic-plastic material. They took constant friction and dilation angles  $\phi$  and  $\psi$  relating them to each other through the stress-dilatancy flow rule of Rowe (1962), by introducing the constant volume friction angle  $\phi_{cv}$ . Since both authors obtained these values of  $\phi$  from plane strain tests, they may be larger than those obtained from conventional triaxial tests.

Fahey and Carter (1993) modelled pressuremeter tests through an axisymmetric plane strain finite element program using a non-linear elastic, Mohr-Coulomb soil model. Their hyperbolic model takes stiffness degradation into account but depends on empirical fitting parameters. The authors demonstrate that no single value of stiffness can realistically reproduce pressuremeter behavior. It should equally be accepted that a single average value of shear modulus taken from the  $G_{ur}$  values measured on a rebound loop will be inadequate to the task of modeling soil-structure interaction problems.

In this paper, the closed form solution of Hughes et al. (1977) has been used to obtain the strength parameters  $\phi$  and  $\psi$  from a pressuremeter test. Fahey and Carter

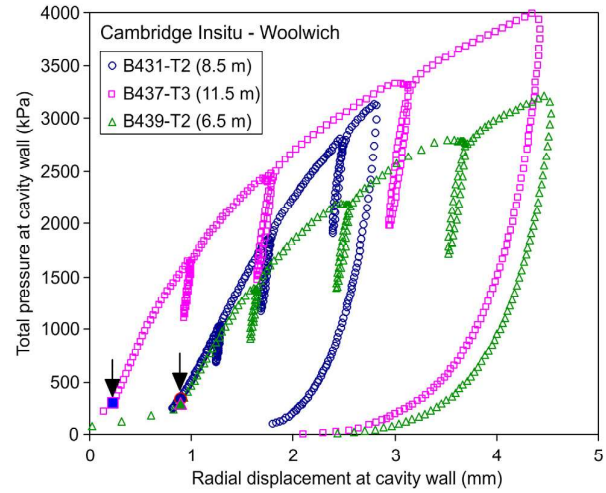


Fig. 3. Field curves of SBP tests at Woolwich

(1993) then offer a useful starting point for the simulation of a pressuremeter test using FLAC3D.

#### 3.2 Modelling pressuremeter tests in FLAC3D

The measured pressure-volume (or radius) responses are related to the shear stiffness and strength properties of the soil. However, these properties are complicated by varying stress and strain conditions around the instrument. This causes difficulties in simulating the whole stress-strain behaviour including unload-reload loops. Fahey and Carter (1993) expended a lot of effort attempting to simulate the expansion and contraction phases of a pressuremeter test but they achieved success only with unload-reload loops. However, they indicated that their main aim, of calibrating the modified hyperbolic model for use in the analysis of geotechnical structures, was not compromised.

This paper follows Fahey and Carter (1993) using a hyperbolic model with a Mohr-Coulomb yield surface to model a pressuremeter test. However, this research used FLAC3D software for the analysis. Furthermore, the hyperbolic model was more sophisticated since it responded to the soil type, soil state and mean effective stress, enabling the evolution of shear modulus during testing. To apply the model and verify its success, three self-boring pressuremeter tests were selected each including three loops. The tests were performed by Cambridge Insitu Ltd and were carried out in the Thanet sand at Woolwich. The curves of pressure versus radial displacement are given in Fig. 3.

Thanet sand is generally described as very dense, grey, silty, quartzitic, fine sand which lies beneath the London clay in central London. Its thickness is around 15 meters (Ventouras, 2005). Since many piled foundations have recently been founded in Thanet sand, a great deal of data has now been collected. For example, Arup Geotechnics (2000) carried out many field test including



self boring pressuremeter tests and pile load tests at Canary Warf. After analyzing their data, they divided the Thanet sand into two sub-strata, the upper stratum of low silt content and the lower stratum of high silt content. Arup Geotechnics (2000) gives corrected SPT  $N_{60}$  values between 30 and 200, voids ratios between 0.65 and 0.95, and fines content between 5% and 30%. Ventouras (2005) explored the engineering properties of this sand from contact core and block samples taken from these two strata and obtained similar index properties. The grading curve envelopes show that the Thanet Sand is mostly very homogenous in its grading and is predominantly fine grained sand, with less than 25% fine material (silt or clay). The author indicated that nature of the Thanet sand is indeed affected to a significant extent by the finest content

The self boring pressuremeter (SBP) aims to minimise soil disturbance. However, after insertion of the SBP into the soil, the membrane may lose contact at some points. Consequently, some initial outward radial movement may be recorded by one of the three or six strain-arms located around the instrument. Radial inward movement of the soil can then occur if the in situ total horizontal stress  $\sigma_{ho}$  is higher than the internal pressure of the membrane at the beginning of the test. The radial stress and soil stiffness may thereby decrease due to the movement of the soil towards the SBP. When the cavity pressure exceeds  $\sigma_{ho}$ , the cavity expands and lift-off occurs. The lift-off pressure gives a rare opportunity to estimate the lateral earth pressure coefficient  $K_o$  which is important for the subsequent finite element analyses. According to Arup Geotechnics (2000), Thanet sand has an overconsolidation ratio changing from 4 to 8 which causes high values of  $K_o$ .

The stiffness decrease which was occurred during initial expansion, may be recovered by a cycle of unloading and reloading. Fig. 4 presents the modeling of a pressuremeter test in FLAC3D. It is essential to define a strain-arm compliance offset  $d$  to capture the initial expansion curve. All observed displacements are reduced by  $d$  and the lift-off pressure is redefined accordingly. In the analysis  $d$  has varied between 0.1 and 0.9 mm, and sometimes it was necessary to reduce the initial value of  $G_o$  by a factor of 0.15 to 0.20.

As demonstrated in Fig. 4, at each reversal of loading, the small-strain shear modulus  $G_o$  is updated using eq. (6) for the points 0 to 7. Updating  $G_o$  only at reversal of loading is similar to the approach applied by Fahey and Carter (1993). The creep stage, which is applied just before reversal of loading, permits static equilibrium to be fully established. It was also needed to reset the shear strain increment ( $ssi$ ), following the reversal of loading at points 1 to 7. For each pressure change (loading stage), the secant shear modulus for each zone is then

calculated using eqs. (2) to (5). All these calculations are carried out by using two FISH functions.

One of the problems with implementing a nonlinear elastic-plastic model is how to vary Poisson's ratio  $\nu$  (or the bulk modulus  $K$ ). Fahey and Carter (1993) indicate that during plastic deformation total volumetric strains are a combination of plastic dilational strains related to plastic shear strain and elastic compression strains related to changes in the mean stress. For Thanet sand it was thought to be appropriate to take  $\nu$  between 0.25–0.45 depending on the content of fines.

For the initial attempts for estimating  $\phi$  and  $\psi$ , the method of Hughes et al (1977) was used. The constant volume friction angle was selected as  $32^\circ$  to  $34^\circ$ . For the further estimates of  $\phi$  and  $\psi$  to capture the field curve, the empirical equation of Bolton (1986) was used:

$$\phi' - 0.8\psi = \phi'_{cv} \quad (11)$$

Fig. 5 shows the simulation of three selected SBP tests at Woolwich (London). The curves given by the best fit (optimized) parameters are compared with the field data. The developed approach is very successful for capturing all the pressuremeter tests. In particular, the modified hyperbolic model has been able quite accurately to reproduce the size and inclination of the loops. The Mohr-Coulomb model came into play for the final unloading phase, and also gave a good fit to the data.

To fully understand the effects on the load-displacement curve of each of the parameters, and to reveal any interchangeability of parameters, more analysis was carried out on test B431-T2 and the results are given in Fig. 6. When the figures are examined, the following interpretations can be made:

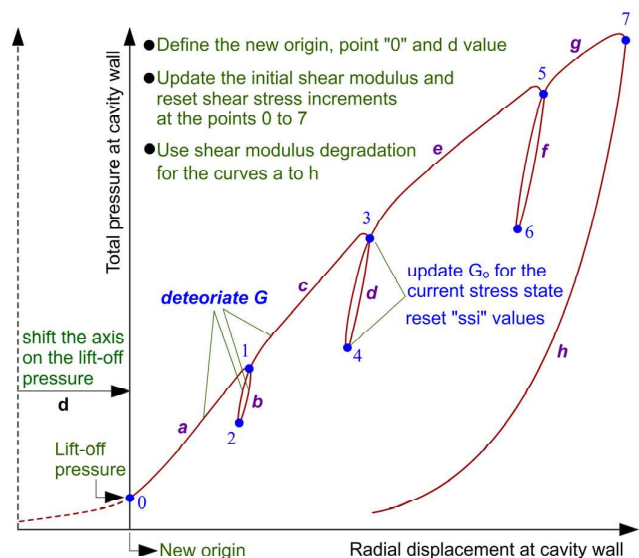


Fig. 4. Presentation of the modelling process in FLAC3D

- $K_o$  affected the whole curve, including the sizes of the loops, but not their inclination. This important parameter can successfully be estimated from the lift-off pressure: (Figs. 6a and 6b).
- The strain-arm compliance offset  $d$  led to improved capture of the first expansion curve of the test. In addition, a reduction was needed in  $G_o$  (Figs. 6c and 6d). These calibrations appeared to give a good representation of the installation effect of a SBP, and may be able to do similarly for pre-bored pressuremeter tests. Fig. 6d demonstrates that the first loop effectively remedies any disturbance effect.
- $G_o$  seems to be the least influential parameter. Using empirical formulation eq. (6) enabled the value to be updated in accordance with the stresses achieved at load reversal. However, any misleading values may have been compensated by other parameters such as  $K_o$ ,  $\nu$  and  $e$ .
- Poisson's ratio  $\nu$  controls elastic compressibility. When it was decreased to 0.25 it should have represented drained behaviour, and when increased to 0.45 undrained behaviour was supposed (Figs. 6e and 6f). Its decrease and increase showed an increasing or decreasing amount of displacement respectively.
- $\phi$  and  $\psi$  showed just the opposite effect of  $\nu$ . So, they could be compensated by  $\nu$ . They define the failure stress, so when they decreased, displacements increased, and when they increased, displacements decreased (Figs. 6g). Fig. 6h interestingly shows the operational equivalence of  $\phi$  and  $\psi$  with  $\nu$ .  $K_o$  and  $\nu$  also presents similar behaviour.
- Fig. 6e and 6j shows how  $e$ ,  $I_D$  and  $U_c$  control the degradation parameters of the modified hyperbolic model;  $\gamma_e$ ,  $\gamma_r$  and  $a$  affect the pressure-displacement curve. Although  $e$ ,  $I_D$  and  $U_c$  have an overall effect on the curve, they affect the small strain range, and especially the size and inclination of the loops. Fig. 6j and 6k demonstrate how loop shape is affected by the degradation of the shear modulus  $G$ .
- If unrepresentative values for  $e$ ,  $I_D$  and  $U_c$  are selected, as seen in Fig. 6k, it is impossible to compensate them with other parameters. In Fig. 6k, it is demonstrated that it is possible to capture the expansion curves well enough; however, the loops are the key factor in calibrating a model and these are now seen to be inadequate. It should be noted that  $\phi=54^\circ$  and  $\psi=29^\circ$  as given in Fig. 6k were calculated by using Hughes et al (1977) for this test curve. But, when the loops are considered, both  $\phi$  and  $\psi$  should be decreased by  $10^\circ$  for optimum overall fit. This result suggests that the low-stress plane strain values of  $\phi$  and  $\psi$  obtained by using Hughes et al (1977) were inappropriate.

- Three different solutions (best fit Fig. 5, Fig. 6h and Fig. 6l) are presented to show that soils can be defined with different combinations of parameters. There are at least 3 ways to successfully simulate this test.

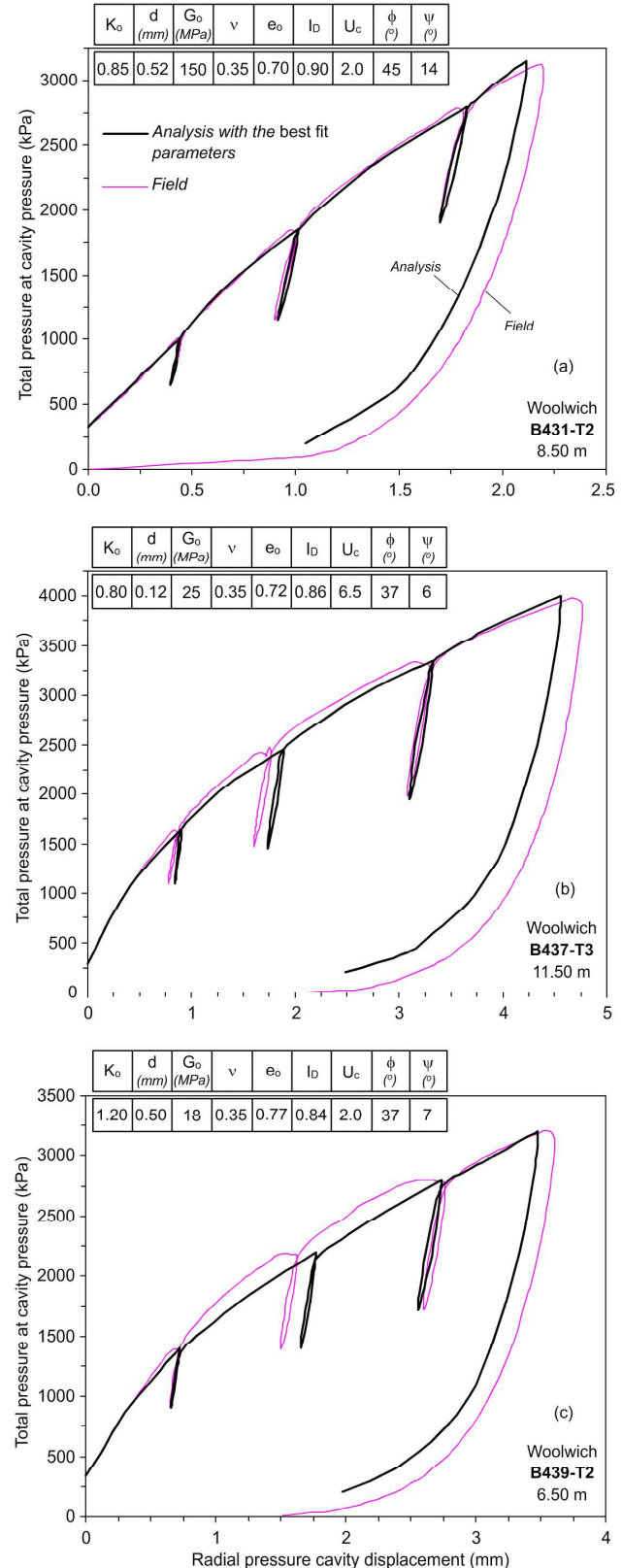


Fig. 5. Best fit curves of SBP tests at Woolwich (a) B431-T2; (b) B437-T3; (c) B439-T2

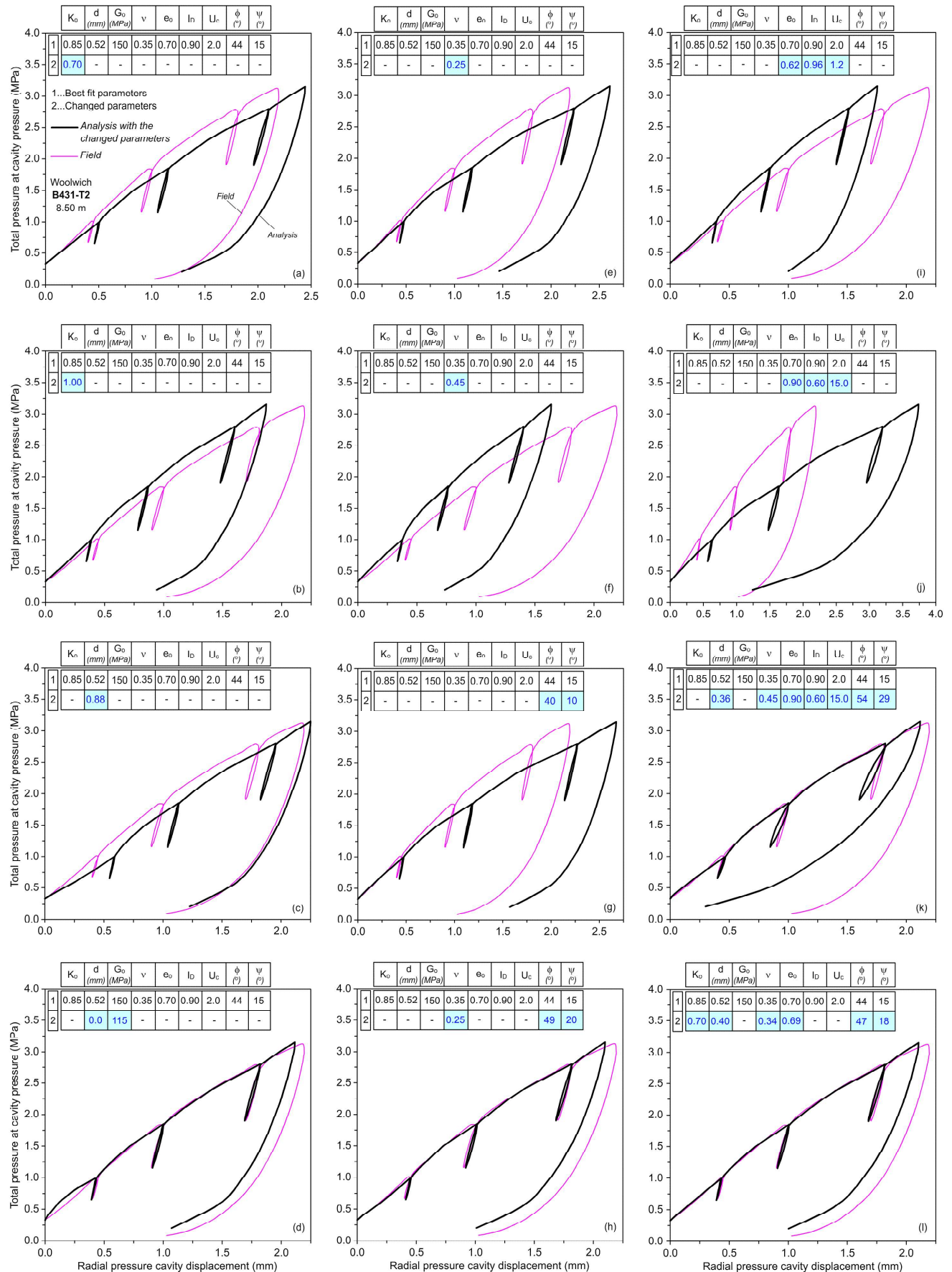


Figure 6. Parameter effect on the presuremeter curve and some examples of parameter combinations (Test: B431-T2)

## 4. CONCLUSIONS

Utilization of a newly developed modified hyperbolic model with the Mohr-Coulomb yield criterion in FLAC3D provides a practical and successful methodology for modelling sands, especially in the small strain range. The model also proved itself for incorporation into numerical analyses.

A SBP test with at least two loops is necessary to implement the proposed approach. In that way, it is easier and more accurate to capture the location of loops, their size, and inclination. The parameters affect the pressuremeter curve in different ways.  $K_o$  affects the whole pressuremeter test curve, including the size of loops.  $G_o$  has a limited affect on the first expansion curve; however, updating it at loops is most important. Poisson's ratio  $\nu$  has a significant impact, similar to  $\phi$  and  $\psi$  but in a reverse sense. So they appear to be interchangeable parameters.  $e$ ,  $I_D$  and  $U_c$  control  $\gamma_e$ ,  $\gamma_r$  and  $\alpha$  which have an overall effect. They especially affect the size and inclination of the unload-reload loops.

It is demonstrated that the degradation of shear modulus is of crucial importance to the simulation of a pressuremeter test. This concept can be extended to the design of geotechnical structures which will be designed for small to medium strains. Since the observed behaviour in a pressuremeter test can be matched by the proposed non-linear model, some confidence may be felt in the use of this calibrated model to predict the behaviour of full-scale geotechnical structures. However, this paper also reveals that a pressuremeter test can be successfully simulated with different combinations of soil parameters. Extra soil test data would assist, as ever.

## ACKNOWLEDGEMENTS

The work was supported by EPSRC Platform Grant GR/T18660/01. The first author was also supported by Scientific Research Projects Coordination Unit of Istanbul University. Project No: BYP-4586. The authors would like to thank to Cambridge Insitu and Dr. Robert Whittle for supplying the pressuremeter data.

## REFERENCES

- Arup Geotechnics (2000). Building HQ1, Factual Geotechnical Information Package, V1-3
- Bolton, M.D. (1986). "The strength and dilatancy of sands," *Géotechnique* 36, No. 1, 65-78
- Darendeli, B.M. (2001). Developpe of a new family of normalizet modulus reduction and material damping curves, Ph. D. dissertation, University of Texas at Austin
- Fahey, M., and Carter, J.P. (1993). "A finite element study of the pressuremeter test in sand using a nonlinear elastic plastic model," *Can. Geotech. J.* 30, 348-362
- FLAC3D (2009). "Fast Lagrangian Analysis of Continua, Manual," Itasca Consulting Group, Minnesota, USA
- Yi, F.F. (2010) "Nonlinear cyclic characteristics of soils" *GeoFlorida 2010: Advances in Analysis, Modeling & Design*, pp. 2601-2610
- Hardin, B.O., and Richart, F.E., (1963). "Elastic Wave Velocities in Granular Soils," *Journal of the Soil Mechanics and Foundation Division* 89, No. SM1, 33-65
- Hardin, B.O. and Drnevich, V.P. (1972). "Shear modulus and damping in soils: design equations and curves," *Journal of Geotechnical Engineering* 98, 667-692
- Hughes, J.M.O, Wroth, C.P., and Windle, D. (1977). "Pressuremeter tests in sands," *Géotechnique* 27, No. 4, 455-477
- Ishibashi, I. and Zhang, X. (1993). "Unified dynamic shear moduli and damping ratios of sand and clay," *Soils and Foundations*, Vol. 33, No. 1, pp.182-191
- Iwasaki, T., Tatsuoaka, F., and Takagi, Y. (1978). "Shear moduli of sands under cyclic torsional shear loading," *Soils and Foundations* 18, No. 1, 39-50
- Jardine, R.J., Potts, D.M., Fourie, A.B., and Burland, J.B. (1986). "Studies of the influence of non-linear stress-strain characteristics in soil-structure interaction," *Geotechnique* 36, No. 3, 377-396
- Kokusho, T. (1980). "Cyclic triaxial test of dynamic soil properties for wide strain range," *Soils and Foundations* 20, No. 2, 45-60
- Mair, R.J. (1993). "Developments in Geotech. Eng. Research: Application to Tunnels and Deep Excavations", Rankine Memorial Lecture 1992 in Proc. of the Institution of Civil Engineers-Civil Engineering, 97, No. 1, 27-41
- Manassero M. (1989). "Stress strain relationships from drained self-boring pressuremeter tests in sands," *Géotechnique* 39, No. 2, 293-307
- Menq, F.Y. (2003). Dynamic properties of sandy and gravelly soils, Ph.D. dissertation, University of Texas at Austin
- Nicholson, D., Chapman, T. & Morrison P. (2002). "Pressuremeter proves its worth in London's Docklands," *Ground Engineering*, March, 32-34
- Oztoprak, S. and Bolton, M.D. (2011). "Stiffness of sands through a laboratory test database," Review process is proceeding in *Géotechnique*.
- Ramberg, W., Osgood, W. R. (1943) "Description of stress-strain curves by three parameters." Technical Note No. 902, National Advisory Commission for Aeronautics
- Rowe, P. W. (1962). The stress-dilatancy relation for static equilibrium of an assembly of particles in contact. *Proc. Roy. Soc., Series A*, 269, 500-527
- Seed, H.B., and Idriss, I.M. (1970). Soil moduli and damping factors for dynamic response analyses, Report EERC 70-10, University of California, Berkeley, CA
- Simpson, B. (1992). Retaining structures: displacement and design. *Geotechnique* 42, No. 4, 541-576
- Tatsuoka, F. and Shibuya, S. (1991). "Deformation properties of soils and rocks from field laboratory tests," *Proc. Of 9<sup>th</sup> Asian Regional Conf. on Soil Mech. and Found. Eng.*, Bangkok, Thailand, 101-170
- Ventouras, K. (2005). Engineering properties of Thanet sand, Ph.D. thesis, Imperial College of Science, Technology & Medicine, London, UK
- Yamashita, S., and Suzuki, T. (1999). "Young's and shear moduli under different principal stress directions of sands," *Pre-failure Def. Charac. of Geomaterials*, Jamiolkovski, Lancellotta & Lo Presti (eds), Balkema, 149-158